Available online at www.sciencedirect.com
ScienceDirect
Journal of Anthropological Archaeology 26 (2007) 517–540
JOURNAL OF Anthropological Archaeology
www.elsevier.com/locate/jaa

Modeling post-depositional mixing of archaeological deposits

P. Jeffrey Brantingham [a,*], Todd A. Surovell [b], Nicole M. Waguespack [b]

[a] Department of Anthropology, University of California, Los Angeles, 341 Haines Hall, Los Angeles, CA 90095, USA
[b] Department of Anthropology, 1000 E. University Avenue, University of Wyoming, Laramie, WY 82071, USA

Received 12 April 2007; revision received 6 August 2007

Abstract

We develop a series of simple mathematical models that describe vertical mixing of archaeological deposits. The models are based on assigning probabilities that single artifact specimens are moved between discrete stratigraphic layers. A recursion relation is then introduced to describe the time evolution of mixing. Simulations are used to show that there may be important regularities that characterize the mixing of archaeological deposits including stages of dissipation, accumulation and equilibration. We discuss the impact of post-depositional mixing on the apparent occupation intensities at modeled stratified archaeological sites. The models may also help clarify some of the problems inherent in making general inferences about the nature culture change based on mixed archaeological deposits. We demonstrate the modeling approach by developing a post-depositional mixing model for the Barger Gulch Folsom site.

Keywords: Post-depositional mixing; Mathematical models; Simulation; Archaeological site formation processes; Folsom

Archaeologists have long-recognized that post-depositional mixing of archaeological deposits may introduce substantial biases into the character of archaeological assemblages (Schiffer 1987; Wood and Johnson 1978). As such, post-depositional mixing may make archaeological inferences problematic, particularly those concerning the nature and pace of culture change (Brantingham, 2007; Lyman 2003; Morin, 2006). In the simplest case, for example, the downwards mixing of archaeological specimens into older deposits could be the source of an erroneous inference that a cultural attribute or behavior appeared earlier than previously thought. Here it is clear that mixing leads to a breakdown of the Law of Superposition. In more realistic situations, where archaeological specimens may be moving *en masse* over long periods of time, the inferential impact may be not only more severe, but also much more complex. For example, the mixing of artifact specimens between discrete stratigraphic units might lead us to question the results of frequency seriation or, indeed, any specific inferences about cultural change than hinge on the relative frequencies of different artifact types.

A battery of methods are available for diagnosing the presence and even severity of post-depositional mixing. These methods fall generally into three categories: (1) comparisons of the degree of overlap in assemblage characteristics based on an

* Corresponding author. Fax: +1 310 206 7833.
E-mail addresses: branting@ucla.edu (P.J. Brantingham), surovell@uwyo.edu (T.A. Surovell), nmwagues@uwyo.edu (N.M. Waguespack).

0278-4165/$ - see front matter
doi:10.1016/j.jaa.2007.08.003

a priori assumption that the pre-taphonomic assemblages were completely non-overlapping in their attributes (Albert et al. 2003; Karavanic and Smith, 1998; Morin et al., 2005; Rowlett and Robbins, 1982); (2) examination of the distribution of refit stone, bone or ceramic specimens between discrete stratigraphic units (Audouze and Enloe, 1997; Bollong, 1994; Delagnes and Roche, 2005; Hofman, 1986; Kroll, 1994; Morin et al., 2005; Surovell et al., 2005; Villa, 1982); and (3) experimental or observational characterization of the behavior of individual taphonomic agents and the development of criteria to aid in recognizing them in the field (Araujo and Marcelino, 2003; Balek, 2002; Bocek, 1986; Erlandson, 1984; Johnson, 1989; Laville et al., 1980; Morin, 2006; Van Nest, 2002). Using the first set of methods, assemblage overlap—for example, in faunal species representation, ceramic or lithic types—is taken as evidence for the presence of post-depositional mixing, but may also serve as a proxy for the magnitude of the disturbance if the degree of overlap can be established. The reliability of the approach is dependent, however, on the validity of the *a priori* models describing the undisturbed assemblage characteristics. The presence of mixing also may be estimated using the second set of methods if there is evidence for refits between discrete stratigraphic units. Here we are often safe in assuming that the specimens comprising a refit set were discarded together and that their separation within a stratigraphic profile is the result of some form of post-depositional mixing. The magnitude of the separation between members of a refit set may provide a measure of the magnitude of mixing (Morin et al., 2005; Villa, 1982), though questions may still remain as to whether a small sample of refits is representative of the disturbance experienced by a much larger assemblage. Using the last collection of methods, mixing is suspected if there is sedimentological or stratigraphic evidence that a specific taphonomic agent such as bio- or cryoturbation has been active at a site. Such suspicions are confirmed with evidence of the preferential orientation of artifacts or specific forms of artifact damage (Esdale et al., 2001; Karavanic and Smith, 1998; Lenoble and Bertran, 2004; McPherron, 2005; Surovell et al., 2005; Villa, 1982). Despite the quantitative nature of these data, however, assessing the magnitude of disturbance using these measure may still be problematic (Lenoble and Bertran 2004).

While these methods are clearly indispensable, it our intention to take a step back from the empirical record to examine the general dynamics of post-depositional mixing. The goal is to provide a simple quantitative basis for describing mixing and lay a foundation for more complex archaeological models. The focus in this paper is on a series of relatively simple mathematical models which describe the mixing of archaeological deposits by a generic post-depositional taphonomic agent. The first section of the paper considers an hypothetical archaeological scenario involving the vertical distribution of artifacts in a sequence of stratigraphic units. The structure of the scenario is meant to be consistent with typical forms of evidence collected in the excavation of archaeological sites, namely three dimensional distribution of archaeological specimens in a stratigraphic section. Drawing on models developed to study sea floor bioturbation and sedimentary diagenesis (e.g., Boudreau, 1997; Meysman et al., 2003; see also Rowlett and Robbins, 1982; Shull, 2001), the components of a discrete mathematical model describing the probabilistic transport of archaeological specimens within a sedimentary profile are presented. Of the formalisms available (see Meysman et al., 2003), discrete transport models are both relatively easy to understand and appropriate for treating distributions of archeological materials in buried contexts. Ordinary and partial differential equation models are preferred for modeling the effects of bioturbation on radioactive tracers (Boudreau, 1997; see also Pendall et al., 1994; Trumbore, 2000), but they also tend to be far more difficult to analyze.

The second section of the paper shows how the basic model components fit together to describe generic post-depositional mixing of archaeological materials between discrete stratigraphic units. The model includes terms to describe the transport of archaeological specimens from one or more stratigraphic units into a so-called focal stratum and transport out of the focal stratum to one or more other stratigraphic units. Key distinctions are made here between local and non-local mixing, on the one hand, and symmetrical and asymmetrical mixing, on the other.

The third section then turns to simulating the impact of different mixing processes on several hypothetical archaeological scenarios. Here we see in a very general, but practical way how post-depositional mixing may impact inferences about temporal patterns of occupation intensity. Local and non-local mixing models are applied to sites that have both single and multiple discrete occupation hori-

zons. A more complex scenario is also examined where mixing is applied to a pre-taphonomic exponential increase in artifact densities meant to mimic a case of increasing occupation intensity at a site. It is shown that there are substantial regularities to the evolution of artifact density profiles in each of these cases, suggesting that the signatures of post-depositional mixing may be both easily recognized and predictable. We consider in the discussion how small sample sizes might impact our ability to recognize these regularities.

The fourth section examines a specific case of mixing at the Barger Gulch Folsom site (Mayer et al., 2005; Surovell et al., 2005; Waguespack, 2005). The simple models developed here provide insights into the nature of post-depositional mixing at Barger Gulch and provide possibly a quantitative basis for estimating the magnitude of disturbance.

The final section of the paper discusses some limitations to and possible extensions of the models. In particular, more complete formal models of archaeological site formation and diagenesis should include a consideration of how site burial, differences in sediment characteristics and variable material characteristics impact mixing. We briefly introduce one such extension where mixing involves a material that degrades through time (e.g., bone).

A model stratigraphic section

Consider a hypothetical stratigraphic section divided into a series of discrete stratigraphic units (Fig. 1a). The stratigraphic units are numbered from bottom to top beginning with Layer 1, which is by definition the base of the sequence. For convenience it is assumed that each stratum is the exact same thickness Δd and each is also identical in terms of sedimentary characteristics. These are simplifications adopted for the purposes of modeling. Archaeological materials may be found buried within any of the strata and a large archaeological site may consist of a number of such stratigraphic sections. In the present case we are not concerned with the initial deposition and burial of archaeological materials in the section, though a more complete model would certainly include these processes. Rather, we are interested only in modeling the process by which materials buried initially within different stratigraphic units may be subsequently transported between units (see Johnson, 1989).

If we start with the assumption that artifacts can only move vertically between stratigraphic units—that is, we do not consider horizontal transport between individual vertical sections—then it is possible to represent the stratigraphic column in Fig. 1a as a one-dimensional line with nodal points for each stratigraphic unit. We label each node with a number corresponding to its stratigraphic layer from 1,2,..., m, where m is the total number of stratigraphic units in a section. In analyzing post-depositional mixing processes between stratigraphic units it will be convenient to talk about movement of specimens into and out of some focal stratum j (Fig. 1b). Other strata in the section may be referred to either in terms of their position relative to the focal stratum (e.g., $j+1$), or using a label $k = 1,2,\ldots,m$, where we are sometimes careful to specify $k \neq j$. The number of specimens of a single artifact class present in a focal stratum j at any point in time is given as n_j and in any other stratum as n_k.

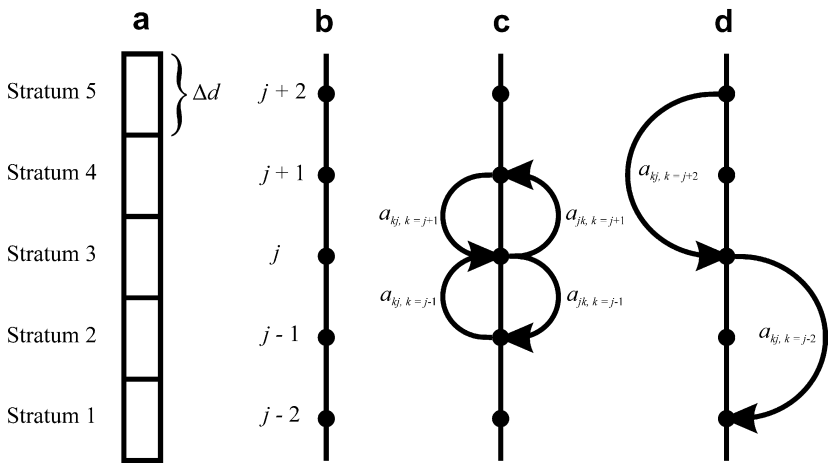

Fig. 1. Hypothetical stratigraphic sequence.

Given this simple mathematical structure, it is possible to model the movement of archaeological specimens between stratigraphic units using so-called hopping probabilities. The probability that any one specimen in a class of artifacts is mixed from the focal stratum, represented by node j, to a different stratum, represented by node k, is given as a_{jk}. The probability that a specimen is mixed from stratum k to the focal stratum j is then a_{kj}. The exact mechanism of transport is intentionally left unspecified so that many different mixing agents might be modeled. For example, a_{jk} might describe the active movement of archaeological specimens between layers by burrowing animals (Erlandson, 1984; Johnson, 1989) or frost heave (Hilton 2003), or passive movement as might occur if archaeological specimens migrate through open cracks or burrows (Johnson, 1989).

For an entire stratigraphic section consisting of m total stratigraphic units, the probabilities that specimens are mixed between any two strata is described by a $m \times m$ transition matrix (Boudreau, 1997; Shull, 2001). For example, for the hypothetical stratigraphic section shown in Fig. 1a, the transition matrix is given as:

$$A = \begin{pmatrix} a_{11} & a_{12} & a_{13} & a_{14} & a_{15} \\ a_{21} & a_{22} & a_{23} & a_{24} & a_{25} \\ a_{31} & a_{32} & a_{33} & a_{33} & a_{34} \\ a_{41} & a_{42} & a_{43} & a_{44} & a_{45} \\ a_{51} & a_{52} & a_{53} & a_{54} & a_{55} \end{pmatrix} \tag{1}$$

The entries in A give the probabilities of movement between any two stratigraphic layers. For example, the row entry a_{21} is the probability that a specimen of a particular artifact class present in stratum $j = 2$ is moved by some taphonomic processes to stratum $k = 1$. Because these are probabilities, the rows (but not necessarily the columns) must sum to one. Note that when $j = k$ the resulting term a_{jk} represents the probability that a specimen remains within the focal stratum. For example, a_{11} is the probability that a specimen of a particular class present in Stratum 1 remains in Stratum 1. In some studies this probability is given as s_j (Shull, 2001) and is calculated as

$$s_j = 1 - \sum_{\substack{k=1 \\ k \neq j}}^{m} a_{jk} \tag{2}$$

The transition matrix given in Eq. (1) may be used to represents both local and non-local mixing of archaeological deposits. Local mixing is said to occur only between adjacent strata. The sediment churning activities of so-called *mixmaster* species, for example, may lead to transfers of materials within and between adjacent strata (Johnson et al., 2005). In Fig. 1c, movement of any specimen from the focal stratum j to either of the adjacent strata $j \pm 1$ is considered local (see Boudreau, 1997). Only the central diagonal and two adjacent diagonals in A have non-zero entries in this case.

By contrast, non-local mixing may occur if any specimen in a stratigraphic layer j can be transported directly to a non-adjacent layer $k > j \pm 1$. Burrowing organisms, for example, may move materials directly between non-adjacent strata producing so-called conveyor-belt mixing (Boudreau, 1997; Johnson et al., 2005). In Fig. 1d, we see a case where specimens from the focal stratum j can be transported directly to a non-adjacent stratum at position $j - 2$, or from stratum $j + 2$ to the focal stratum. The transition matrix in this case would have additional entries beyond the main diagonal and those immediately above and below. Note, however, that non-local mixing is not the only mechanism by which archaeological specimens can make their way from a focal stratum to non-adjacent layers. Local mixing may lead to the movement of specimens between non-adjacent strata over time. For example, if a specimen was initially deposited in a stratum j and at some point was mixed to the next lower stratum in the section $j - 1$, then this same specimen might at some later time be mixed from stratum $j - 1$ to the next lowest stratum, $j - 2$. If we were to follow this specimen over the course of many time steps the process of stratigraphic mixing would be described as Markovian. In other words, the location of the specimen at time t is dependent only upon its location at time $t - 1$ and the associated probabilities of mixing between stratigraphic units. In the case of strict local mixing, over time a specimen may migrate from one stratum into non-adjacent strata through one or more intermediate transport events. The time dynamic of mixing is a simple random walk between layers.

Modeling mass movement

To model the movement of multiple archaeological specimens out of a focal stratigraphic unit j we define $a_{jk} n_j$ as the total number of specimens leaving j and being deposited in stratum k in a single mixing event (Boudreau, 1997; Meysman et al., 2003). The expected number of specimens being moved to all

other strata $k = 1,2,\ldots, m$ from stratum j in a single event is then

$$E[n_{jk}] = n_j \sum_{\substack{k=1 \\ k\neq j}}^{m} a_{jk} \tag{3}$$

Similarly, to model the movement of multiple specimens into the focal stratigraphic unit we first define $a_{kj}n_k$ as the total number of specimens moving from any other stratum k to stratum j. The expected number of specimens moving into j in a single event is then given by

$$E[n_{kj}] = \sum_{\substack{k=1 \\ k\neq j}}^{m} a_{kj}n_k \tag{4}$$

It is important in both Eqs. (3) and (4) to specify that the sums are taken over all stratigraphic units excluding the focal unit (i.e., $j \neq k$). This ensures that the equations refer exclusively to taphonomic mixing between layers, rather than mixing within layers. This is a distinction that is sometimes made in identifying post-depositional mixing using refit stone or bone specimens (Morin et al. 2005).

Given these components it is possible to write a recursion relation to study the time evolution of the number of specimens of a given class of artifact present in a focal stratigraphic layer

$$n'_j = n_j + \Delta n_j \tag{5}$$

Eq. (5) states that the number of specimens in the focal stratum in the next time interval n'_j (the prime indicating a that a change has occurred) is simply the number of specimens in the previous time step n_j plus any change Δn_j in the number of specimens through taphonomic mixing. Using Eqs. (3) and (4) we can write

$$\Delta n_j = \underbrace{\sum_{\substack{k=1 \\ k\neq j}}^{m} a_{kj}n_k}_{\text{transport in}} - \underbrace{n_j \sum_{\substack{k=1 \\ k\neq j}}^{m} a_{jk}}_{\text{transport out}} \tag{6}$$

giving the master equation

$$n'_j = n_j + \sum_{\substack{k=1 \\ k\neq j}}^{m} a_{kj}n_k - n_j \sum_{\substack{k=1 \\ k\neq j}}^{m} a_{jk} \tag{7}$$

The second and third terms on the right hand side of Eq. (7) give some clues to the dynamics of taphonomic mixing. The second term is always greater than or equal to zero and therefore will tend to increase the number of specimens of a given class of artifact within the focal stratum j. By contrast, the third term is always less than or equal to zero and therefore will tend to decrease the number of specimens represented in the focal stratum j.

Simulated post-depositional mixing

It is reasonably straightforward to simulate the effects of post-depositional mixing on archaeological deposits by iterating Eq. (7) and using a transition matrix like Eq. (1) defined *a priori*. Here we consider several baseline cases including: (1) symmetrical local and non-local mixing, where the probabilities of mixing upward through a stratigraphic section are the same as mixing downward; (2) asymmetrical local mixing, where the probability of mixing downward through the section is greater than upward; (3) local and non-local mixing of two discrete occupations; and (4) local mixing of an exponentially increasing occupation. The baseline cases are not meant to be exhaustive, nor are they tied to any specific archaeological case. Rather they serve to illustrate some of the general dynamics and patterns that may result from post-depositional mixing.

All of the simulation models have several properties in common. First, the models examine an hypothetical stratigraphic profile with 51 discrete stratigraphic units or layers (Fig. 2). Mixing dynamics are therefore described by a 51×51 transition matrix. All stratigraphic units are of the same thickness and composition, a simplifying assumption of the abstract specification above. The models are not dependent upon adhering to these properties, however (see Boudreau, 1997; Meysman et al., 2003; Shull, 2001). Stratum 1 is at the base of the profile and is assumed to be above sediment or bedrock that is impermeable to post-depositional mixing. Stratum 51 is the unit directly below the sediment–surface interface. It is assumed that there is no mixing of archaeological materials between the surface and subsurface.

In all of the following simulations the number of specimens within each stratigraphic unit is measured in discrete vertical sections at points distributed along the length of the profile. These vertical sections might be regularly spaced, as is frequently the case when excavating a site using a sampling gird. In the present case there are 100 randomly distributed vertical sections along the simulated stratigraphic profile. Given such a large sample of

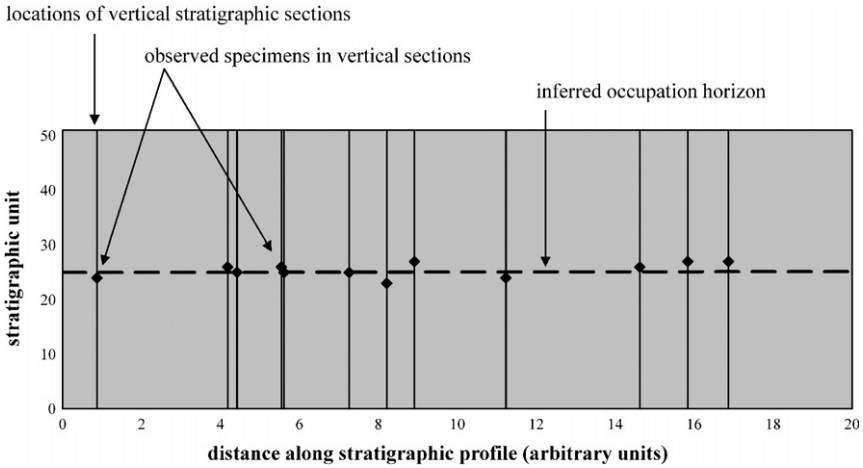

Fig. 2. A stratigraphic profile showing the basic elements of the simulations.

vertical artifact densities it is generally possible to infer the profile-wide distribution of archaeological materials. In Fig. 2, the distribution of artifacts observed in 20 of the 100 randomly spaced vertical sections leads the inference that there is a single, compact occupation horizon centered around Stratum 25.

Since the initial distribution of archaeological materials in the simulated stratigraphic section is known *a priori* it is possible to look at a number of different measures of how post-depositional mixing impacts the character of archaeological deposits. First, in some cases we are interested in the change in the mean stratigraphic position (depth) of an archaeological occupation through multiple stages of post-depositional mixing. This measure is particularly relevant for tracking the impact of mixing on archaeological deposits that were initially unimodal; i.e., deposits that display only one density peak in the section. Second, we are also interested in how specimens are spread throughout a stratigraphic section over the course of mixing. Here we consider changes in the standard deviation of the distribution of specimens across stratigraphic units and the maximum distances over which individual specimens are mixed. Finally, we ask whether there are distinct stages that a deposit goes through during mixing.

Simple mixing scenarios

Symmetrical local mixing

The simplest possible mixing scenario to consider is symmetrical local mixing of a discrete occupation. Here we begin with artifacts buried within Stratum 25 and observed in each of 100 vertical sections along the profile. For simplicity there are initially 20 specimens in each of the 100 sections giving a total of 2000 specimens for the entire profile. Mixing is both symmetrical and local, meaning that the probabilities of mixing upward and downward in the stratigraphic column are equal and that individual specimens can move only to immediately adjacent stratigraphic units. More specifically, the probability that a single specimen moves up or down one stratigraphic unit in a single time step is $a_{jk} = 0.01$, when $k = j \pm 1$. Mixing to non-adjacent strata is prohibited so that $a_{jk} = 0$, when $k > j \pm 1$. The probability that a specimen remains in place during a single time step is $s_j = 1 - \sum a_{jk,\ k \neq j} = 0.98$. These terms comprise a transition matrix with a main diagonal set of entries and diagonals above and below. All other entries in the matrix are zero.

Fig. 3 shows the distribution of archaeological specimens across the 51 hypothetical stratigraphic units after post-depositional mixing lasting different lengths of time. Prior to mixing all of the specimens are contained within Stratum 25, as shown by the single frequency spike at time step zero. With the start of mixing, specimens begin to migrate to positions above and below the original occupation horizon and within 50 time steps more than half of the specimens are found outside of their original stratigraphic unit. The maximum displacement after 50 time steps is ~4 stratigraphic units above and below, demonstrating that repeated local mixing can lead to migration of artifacts between non-adja-

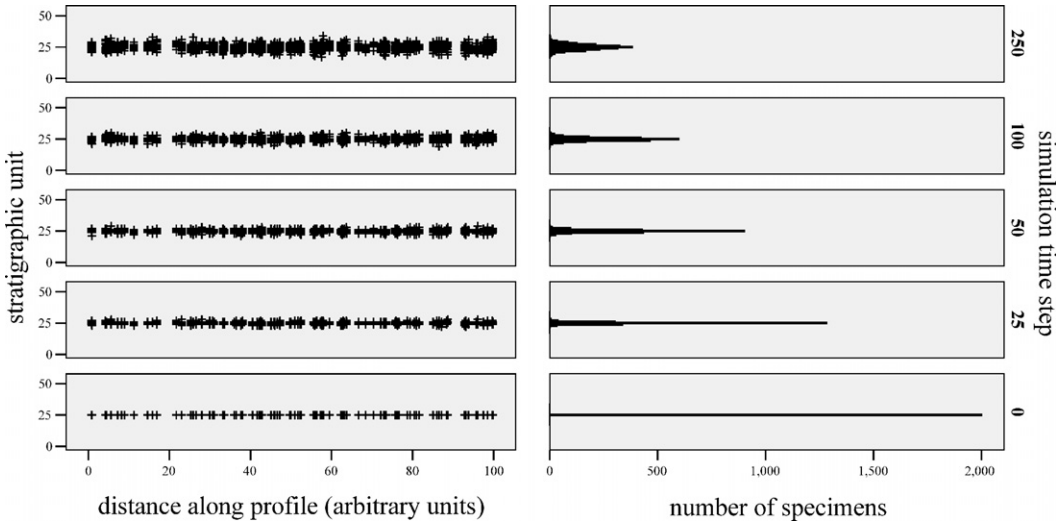

Fig. 3. Symmetrical local mixing of a single occupation horizon over a short period of time. The panels on the left show the vertical position of observed specimens along the face of the profile before taphonomic mixing (bottom) and after 25, 50, 100 and 250 simulation time steps. The panels on the right show the frequency distribution of all specimens across all strata for the same times.

cent strata (Table 1). The original occupation horizon continues to lose specimens and the distribution of artifacts across the strata approaches a symmetrical Gaussian form, which is particularly evident by 250 time steps. At this point, the maximum displacement of specimens from their original depositional context is ~9 units above and below and 35% of the stratigraphic units (18 of 51) contain specimens mixed from the original layer. Not surprisingly, the standard deviation of the distribution of specimens across strata increases with mixing (Table 1). The mean stratigraphic position, however, remains approximately stationary.

As Fig. 4 makes clear, however, a symmetrical, Gaussian distribution of specimens is only characteristic of symmetrical local mixing over relatively short time periods. The actual equilibrium state of the system is a uniform distribution of specimens across all stratigraphic units. The pronounced mode apparent in the distribution of specimens after limited mixing dissipates and is difficult to identify after 10,000 simulation time steps. At 25,000 time steps we approach maximum variance in the distribution, but the mean remains at the center of the profile (Table 1). The maximum displacement of any one specimen from the original depositional context is 25 layers.

Asymmetrical local mixing

If there is a bias in the movement of archaeological specimens towards positions farther down (or farther up) a stratigraphic profile, then we are dealing with asymmetrical mixing. If this mixing is also local, meaning that movement of specimens is only between adjacent stratigraphic units, then it is relatively straightforward to modify the above model to deal with the asymmetrical case. Fig. 5 illustrates a mixing system where the probability that a single archaeological specimen is mixed from a focal stratum j to the next lower stratum $k = j - 1$ is $a_{jk} = 0.04$. The probability of mixing from j to the next higher stratum $k = j + 1$ is $a_{jk} = 0.01$. There is thus a weak bias for downward mixing. Over the short term, specimens spread out from the original occupation horizon. The observed distribution after 250 simulation time steps is skewed towards higher stratigraphic levels, though it is still visually similar to a Gaussian normal distribution. Greater biases in the probability of downward mixing tend to enhance the skew (e.g., Morin 2006). What is also apparent, in contrast with symmetrical local mixing, is that the distribution migrates down the profile. The mean stratigraphic position of all specimens declines from Stratum 24, after 25 simulation time steps, to Stratum 7, after 250 simulation time steps (Table 1). The variance and maximum deviations from the original occupation horizon also increase. After 250 simulation time steps, 23 stratigraphic units separate the uppermost and lowermost specimens and the maximum deviation from the original occupation horizon is ~25 layers. Eventually this pattern is reversed and the variance and maximum

Table 1
Summary statistics for mixing models involving a single initial occupation horizon

Simulation time step	Mean stratigraphic position	Standard deviation	Minimum stratigraphic position	Maximum stratigraphic position
Symmetrical local mixing of a single occupation				
0	25.00	0.00	25	25
25	24.99	0.70	22	28
50	24.97	1.01	21	29
100	25.01	1.44	19	30
250	24.97	2.27	17	34
500	24.92	3.17	14	37
1000	24.91	4.54	9	39
5000	24.62	10.04	1	51
25,000	23.99	12.57	1	51
20,000	23.92	14.40	1	51
Asymmetrical local mixing of a single occupation horizon				
0	25.00	0.00	25	25
25	24.19	1.16	19	28
50	23.44	1.60	17	29
100	21.84	2.28	12	29
250	17.04	3.57	5	28
500	9.29	4.79	1	27
1000	1.78	1.75	1	21
5000	1.31	0.64	1	6
Symmetrical non-local mixing of a single occupation horizon				
0	25.00	0.00	25	25
25	24.79	0.00	6	44
50	24.79	6.10	3	50
100	24.47	8.62	1	51
500	24.37	13.75	1	51

deviations decrease as more and more specimens accumulate at the base of the section (Fig. 6 and Table 1). There is a trailing "tail" of specimens maintained in a few strata above the base of the section by the small probability of upward movement of specimens. Mixing continues, but the distribution is stationary.

More complex mixing scenarios

Symmetrical non-local mixing

Non-local mixing by definition involves the movement of specimens directly between non-adjacent strata. To model such systems it is necessary to define transition probabilities a_{jk} (and a_{kj}) for $k > j \pm 1$. There are many possible ways in which we could define these probabilities. Illustrative in the present case is to make the transition probabilities between a focal stratum j and another non-local stratum k a function of the distance between the strata

$$a_{jk} = a_{jl} d^{-\mu}, \quad l = j \pm 1 \text{ and } k = j \pm d \tag{8}$$

Here stratum k is located d strata above or below the focal stratum j, a_{jl} is the baseline local mixing probability and μ is an constant that falls in the range $1 < \mu \leqslant 3$ (see also Reible and Mohanty, 2002). Note that because the strata are all of equal thickness d is a ratio scale metric. Eq. (8) states that the probability that a single specimen mixes between any two strata is a negative power of the distance between them (Fig. 7). In general, most mixing events are between adjacent strata but occasionally there are mixing events over longer distances between non-adjacent strata. Note that when $d = 1$, Eq. (8) returns the local mixing probability (i.e., $a_{jk} = a_{jl}$), which from the symmetrical case above is 0.01. When $d > 1$ the probability of mixing between layers declines rapidly, but over many mixing events even low probability will tend to occur. For example, with $\mu = 1.2$ and the local mixing probability $a_{jl} = 0.01$, the movement of a specimen from Stratum 25 to Stratum 15 (i.e., $d = 10$) is expected to occur with a probability $a_{jk} = 0.006$, or approximately once every 1667 mixing events.

Fig. 8 shows the results of non-local mixing in our hypothetical stratigraphic profile when

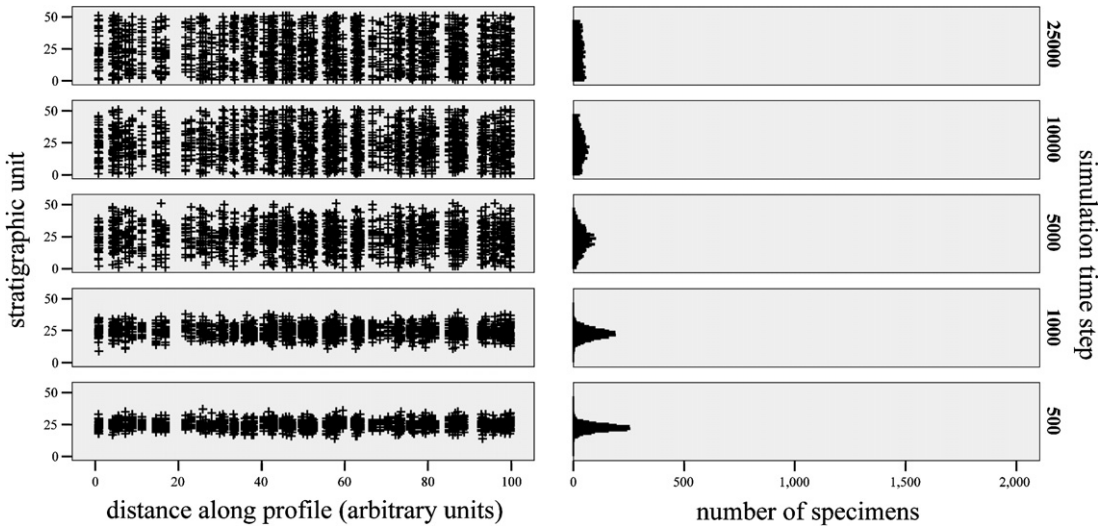

Fig. 4. Symmetrical local mixing of a single occupation horizon over a long period of time. The panels on the left show the vertical position of observed specimens along the face of the profile after 500, 1000, 5000, 10,000 and 25,000 simulation time steps. The panels on the right show the frequency distribution of all specimens across all strata for the same times.

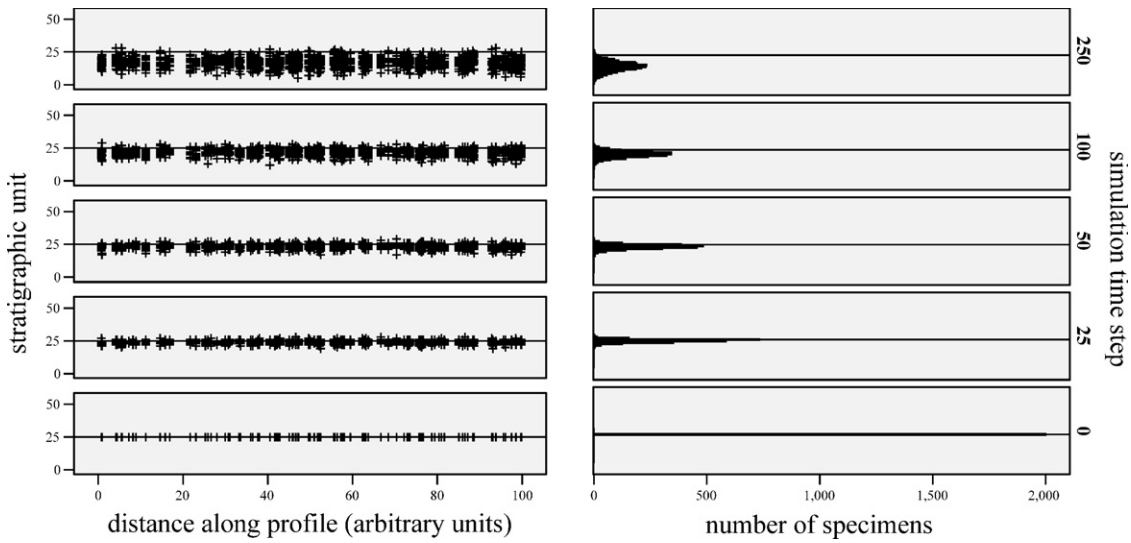

Fig. 5. Asymmetrical local mixing of a single occupation horizon over a short period of time. The panels on the left show the vertical position of observed specimens along the face of the profile before taphonomic mixing (bottom) and after 25, 50, 100 and 250 simulation time steps. The panels on the right show the frequency distribution of all specimens across all strata for the same times.

$a_{jl} = 0.01$ and $\mu = 1.2$. The broad dynamics of the system are the same as for local mixing, namely that specimens from the original occupation horizon in Stratum 25 spread out to form a unimodal distribution and then ultimately converge on a uniform distribution across all strata. However, there are several important quantitative differences with non-local mixing. First, compared with the Gaussian distribution seen with local mixing, the non-local mixing distribution is initially strongly concave with long tails. In fact, very early in the process of mixing, at 25 time steps, the distribution of specimens above and below the original occupation horizon follows approximately the probability distribution shown in Fig. 7. The maximum displacement of specimens from the original occupation horizon after 25 time steps is ~19 stratigraphic layers and the maximum separation

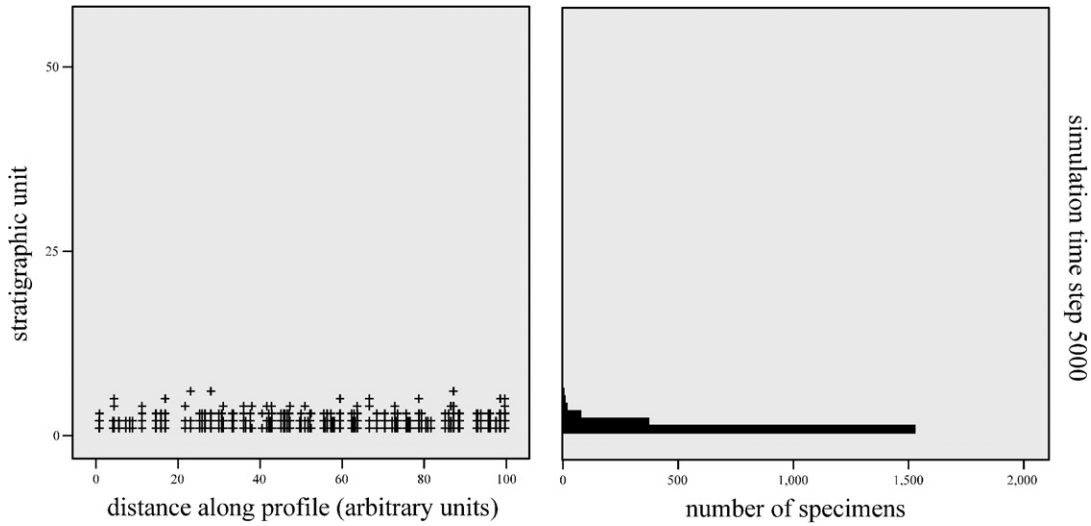

Fig. 6. Asymmetrical local mixing of a single occupation horizon over a long period of time. Shown on the left is the vertical position of observed specimens along the face of the profile after 5000 time steps of simulated mixing. The panel on the right shows the frequency distribution of all specimens across all strata for the same mixing period.

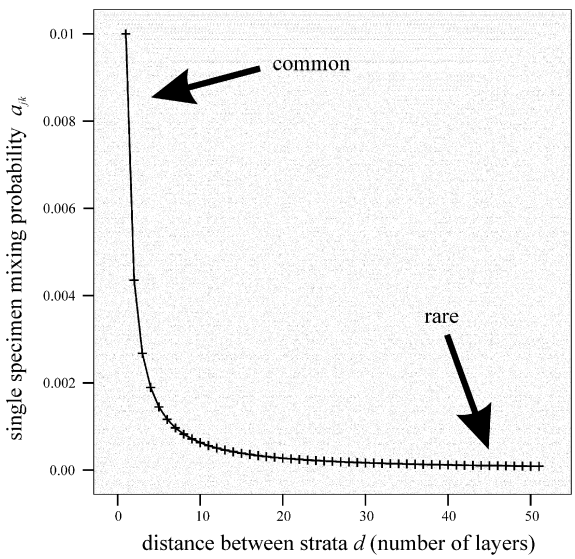

Fig. 7. A Lévy distribution describing the probability of mixing between adjacent and non-adjacent stratigraphic units.

of any two specimens is 38 stratigraphic layers (Table 1). Second, by 100 time steps, the distribution appears more Gaussian-like in shape, though the standard deviation of the distribution (non-local: $\sigma = 8.62$) is approximately six times larger than with local mixing at the same time step (local: $\sigma = 1.44$). Third, the system approaches a uniform distribution at much faster rate, 500 simulation time steps compared with the ~25,000 time steps it took with local mixing.

Local and non-local mixing of two discrete occupations

Arguably, post-depositional mixing of a single discrete occupation only tends to impact our perception of the duration and intensity of occupation. While the associated dynamics are important to understand, they do not necessarily provide obvious expectations for what happens in mixing multiple discrete occupations. Consider a case of symmetrical local mixing identical to that described above, but here starting with two discrete occupations located in strata 17 and 34, respectively (Fig. 9). A total of 18 stratigraphic layers separate the two occupations prior to mixing. Ten specimens are observed in each horizon in each of the 100 randomly spaced vertical sections (see Fig. 2). Thus, the sampled horizons each contain 1000 specimens and combined have 2000 specimens. With the onset of mixing, specimens begin to spread out from each of the discrete occupations in a manner identical to the single occupation case discussed above. Both are approximately Gaussian and the means of each remain centered on the original occupation strata. However, the tails of the distribution start to approach one another and, within 250 simulation time steps, specimens that have migrated down-

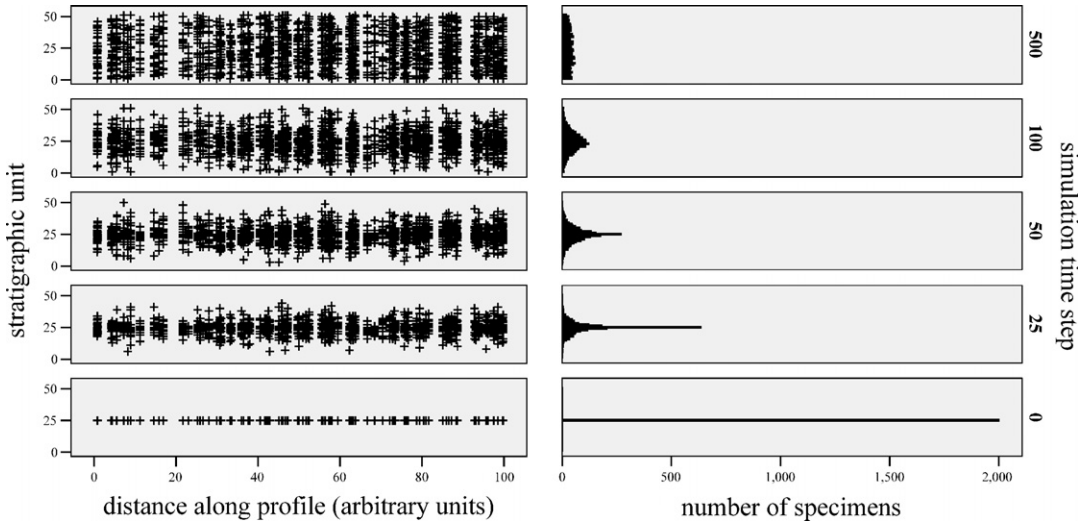

Fig. 8. Symmetrical non-local mixing of a single occupation horizon over a short period of time. The panels on the left show the vertical positions of observed specimens along the face of the profile before taphonomic mixing (bottom) and after 25, 50, 100 and 500 simulation time steps. The panels on the right show the frequency distribution of all specimens across all strata for the same times. The probability of mixing between layers is calculated from Eq. (8) with $a_{jl} = 0.01$ and $\mu = 1.2$.

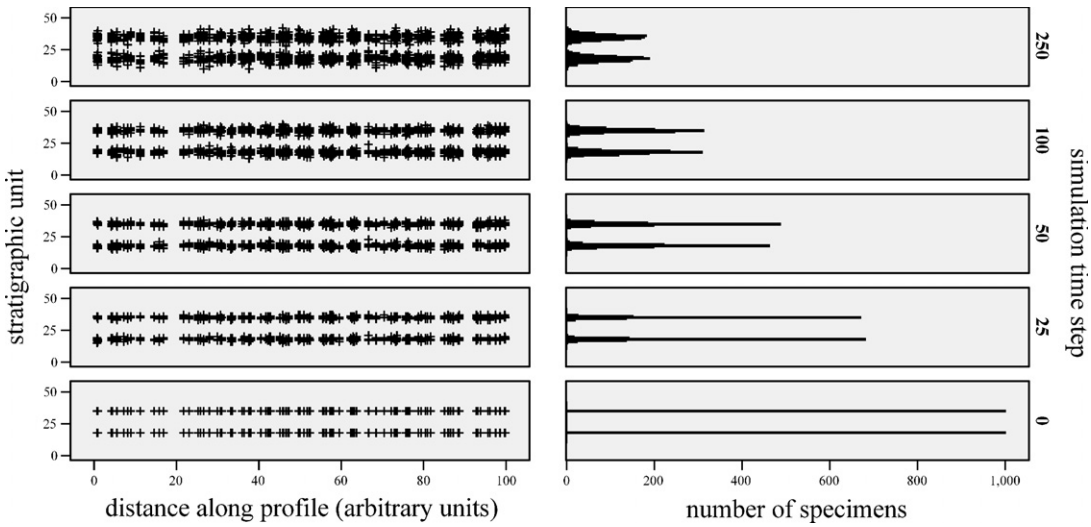

Fig. 9. Symmetrical local mixing of two discrete occupations located initially in strata 17 and 34. The panels on the left show the vertical positions of observed specimens along the face of the profile before taphonomic mixing (bottom) and after 25, 50, 100 and 250 simulation time steps. Each occupation horizon originally contained ten specimens at each of the measured vertical sections. The panels on the right show the frequency distribution of all specimens across all strata for the same times.

wards from the upper occupation are found in the same strata as specimens that have migrated upwards from the lower occupation (Fig. 9). At this point, the distributions are no longer discrete, or non-overlapping. In a strict sense, the stratigraphic sequence appears to contain a continuous occupation with a bimodal distribution of occupation intensities.

Fig. 10 illustrates that, as mixing continues, the two distinct modes gradually disappear and, by time step 5000, merge into a unimodal distribution with a mean centered midway between the two original occupation horizons. By this point specimens have also migrated to the top and bottom of the stratigraphic section. After time step 5000, the single mode begins to dissipate and the frequency of spec-

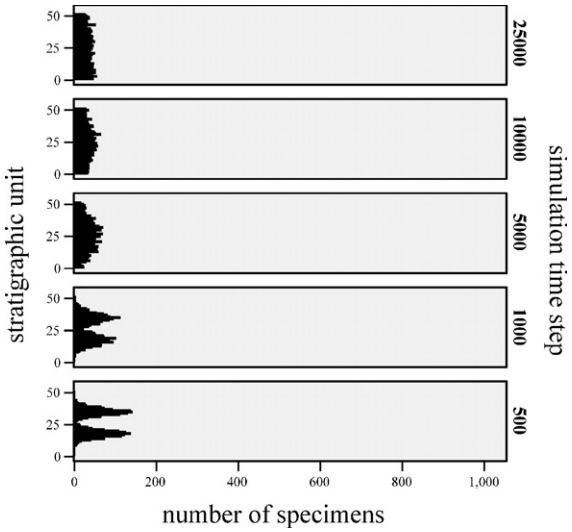

Fig. 10. Symmetrical local mixing of two discrete occupation horizons at 500, 1000, 5000, 10,000 and 25,000 simulation time steps. Shown are the frequency distributions of all specimens across all strata for each time step.

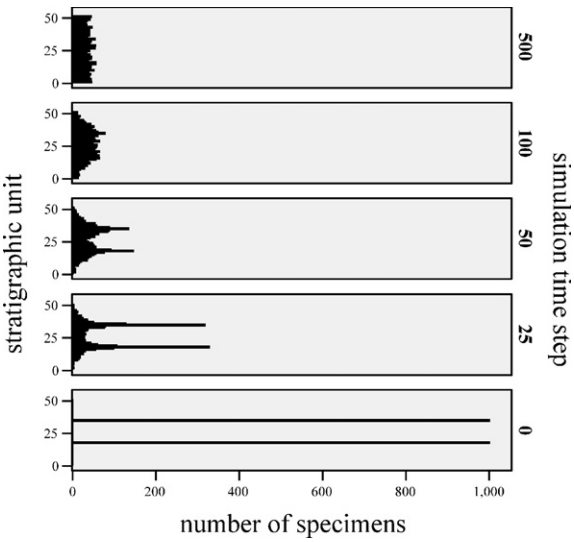

Fig. 11. Symmetrical non-local mixing of two discrete occupations located initially in strata 17 and 34. Each occupation horizon contains ten specimens at each of the measured vertical sections. Shown are the frequency distribution of all specimens across all strata before taphonomic mixing (bottom) and after 25, 50, 100 and 500 simulation time steps.

imens across all stratigraphic levels converges on a uniform distribution. The endpoint of this process involving two discrete occupation horizons is indistinguishable from the case involving one discrete occupation horizon (compare Fig. 4 and 10).

The same general conclusion may be drawn about non-local mixing of two discrete occupation horizons (Fig. 11). Using the parameters for non-local mixing employed above, it is clear that the two discrete occupations follow the trajectory of a single occupation during the early stages of mixing (compare with Fig. 8), namely the development of strongly "peaked" and concave distributions centered on the original occupations. The two modes eventually merge to form a single unimodal distribution, occurring here at around 100 simulation time steps. Eventually the single mode dissipates to form a uniform distribution of archaeological specimens across all strata. The time to arrive at a uniform distribution (~500 simulation time steps) is again much faster compared with local mixing (~25,000 simulation time steps) (compare Fig. 10 and 11).

Local mixing of an exponentially increasing occupation

A final hypothetical case to examine involves a pre-taphonomic occupation that spans strata 10 through 40. The occupation is characterized by an exponentially increasing numbers of specimens from two specimens observed in Stratum 10 up to 22 specimens in Stratum 40 in each of the vertical sections (Fig. 12). Above Stratum 40 the number of specimens drops to zero. This is a vertical distribution of artifacts that one might expect if occupation intensity was increasing through time followed by site abandonment at the peak of occupation (but see Surovell and Brantingham, 2007).

Symmetrical local mixing using the parameter values introduced above eventually eradicates any trace of the initial exponential occupation pattern and rapid site abandonment (Fig. 12). By time step 5000, the occupation appears to increase and then decrease smoothly through time. The mode of the distribution is also displaced downwards in the section such that the apparent peak of occupation intensity at time step 5000 is in Stratum 34, as opposed to Stratum 40 before mixing. As was the case in all of the other examples of symmetrical mixing presented above, the representation of specimens across all strata ultimately converges on a uniform distribution, seen clearly in simulation time step 25,000. Occupation intensity appears to remain constant through time.

Vertical mixing at the Barger Gulch Folsom site

We demonstrate how to develop and apply a general mixing model like those presented above using

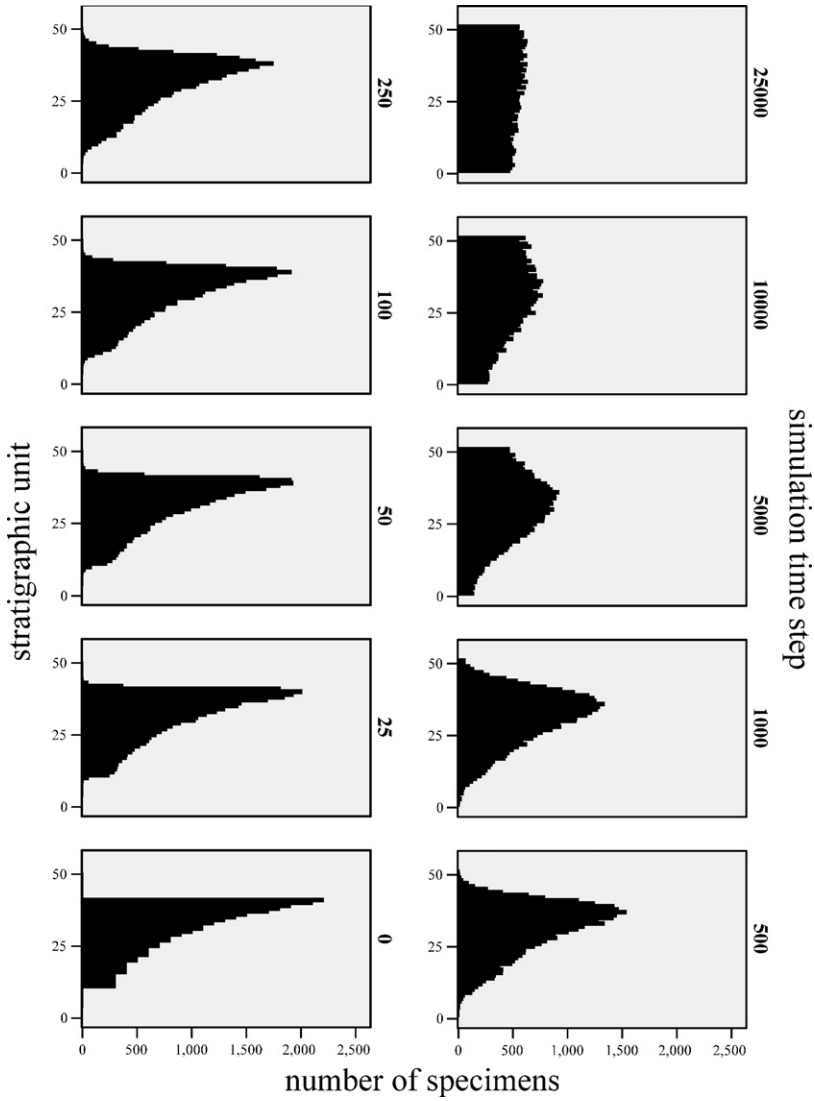

Fig. 12. Symmetrical local mixing of an occupation that is originally distributed across strata 10 to 40 and exponentially increasing through time. Shown are the frequency distributions of archaeological specimens across all strata before post-depositional mixing (bottom left), after 25, 50, 100, 250 (left panels), and after 500, 1000, 5000, 10,000, and 25,000 simulation time steps (right panels).

data from the Barger Gulch site, a series of late Pleistocene and early Holocene archaeological localities associated with Barger Gulch, a tributary of the Colorado River in Middle Park, Colorado (USA). Since 1997, the University of Wyoming has completed eight seasons of excavation at Locality B, a large single component Folsom campsite (Kornfeld and Frison 2000; Kornfeld et al. 2001; Mayer et al. 2005; Surovell et al., 2005; Waguespack et al., 2006). Through the 2006 field season, more than 60,000 chipped stone artifacts have been recovered and more than 12,000 of these have been mapped with mm precision in three dimensions. Spatial data from the site provide an excellent case for evaluating the potential of the above models to replicate a real-world vertical artifact distributions.

Chipped stone artifacts are found in relatively discrete clusters associated with hearth features (Surovell and Waguespack, in press; Waguespack et al., 2006). Stratigraphically, the Barger Gulch Folsom occupation is shallowly (0–60 cm) buried in primary/and or secondary aeolian sediments heavily modified by pedogenesis (Surovell et al., 2005). It is extremely difficult to identify lithostratigraphic units at the site since all sediments are texturally similar (silt loam), and therefore stratigraphic

designations are based in large part on pedostratigraphy (Surovell et al., 2005). Detailed descriptions of stratigraphy and post-depositional artifact dispersal can be found in Surovell et al. (2005) and Mayer et al. (2005), and only a brief summary of the geomorphic history of the site is provided here.

Aeolian silts began slowly aggrading on a lag surface of Miocene bedrock residuum in the late Pleistocene. The ground surface was slowly aggrading or relatively stable at the time of human occupation (ca. 10,450 ^{14}C yr BP) because the occupation surface is associated with the upper contact of a well developed Btkb soil horizon. Following the occupation, the site experienced mild erosion, stripping the A horizon of the Pleistocene soil. Deposition resumed by 9400 ^{14}C yr BP. During the early Holocene as much as 40–50 cm of silt accumulated burying the Folsom occupation. During the early to middle Holocene, the surface stabilized and a well developed soil formed. In the late Holocene, this soil was partially truncated by erosion and then buried by up to 30 cm of silt loam. Although stratigraphic sections across the site are fairly consistent, the magnitude of erosion and soil formation varies laterally.

In Fig. 13, we present five randomly chosen vertical artifact distributions from the site. Each graph shows lithic artifact counts by 5 cm excavation level for individual 1 m^2 excavation unit. Artifacts are generally found throughout the late Quaternary deposits. In typical excavation units (e.g., Fig. 13b–e), artifact counts gradually increase from the surface downward reaching their maximum at what we interpret to be the Folsom occupation surface. Below the occupation horizon, artifact counts rapidly drop to zero, usually within 10–15 cm. In roughly 10% of excavation units, vertical artifact distributions show considerably more noise and/or multimodality (e.g., Fig. 13a). When viewed in cross-section, the zone of high artifact density marking the Folsom occupation surface is evident with considerable movement of artifacts upward and minimal downward movement (Fig. 14).

Producing a general vertical artifact density distribution for the entire site requires standardizing absolute artifact elevations to a common stratigraphic unit. The most readily identifiable depositional event at the site is the Folsom occupation itself. Thus, artifact elevations by excavation unit were standardized to the Folsom occupation surface, identified as a weighted (by artifact count) average of elevation for the three contiguous 5 cm levels with the greatest artifact count. We are confident that this method accurately identifies the occupation surface. This surface is consistently associated with the largest artifacts (>100 g), which should be least likely to experience post-depositional movement, and it is bracketed by radiocarbon ages which place it in the correct time frame for a Folsom occupation (Surovell et al., 2005). Finally, pit and hearth features originating from this surface have been identified (Surovell et al., 2005; Waguespack et al., 2006). For the purposes of this

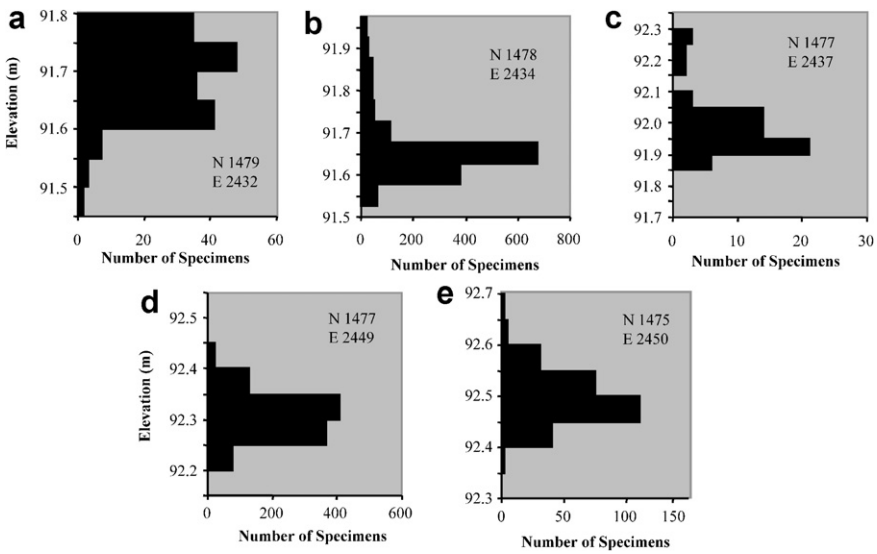

Fig. 13. Vertical distribution of lithic specimens in five randomly chosen excavation units at the Barger Gulch Folsom site.

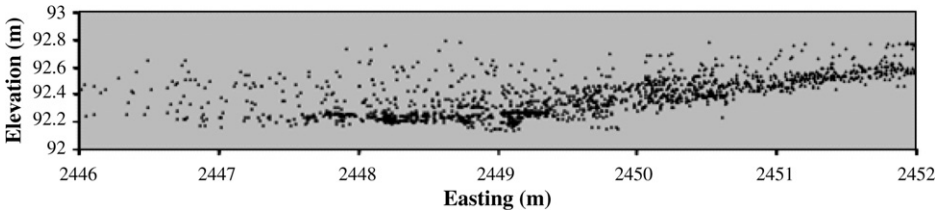

Fig. 14. Composite profile of the Barger Gulch site showing the vertical and horizontal distribution of lithic specimens for a 1 m thick transect through on portion of the site from N1474 to N1475.

paper, it is of no consequence that the original Folsom occupation surface may have been somewhat deflated by erosion, since the resulting lag would have been a single surface with a vertically constrained distribution at the time of burial.

To minimize the effects of size-dependent mixing, we limit this to analysis to piece-plotted lithic artifacts with maximum length of 10–25 mm (Surovell et al., 2005). This includes a total of 7018 specimens from the 75 m^2 excavated area. The composite vertical distribution of artifacts at the site is shown in Fig. 15. The distribution in unimodal with the upper and lower tails both strongly concave. The upper tail of the distribution is much longer than the lower tail towards the base of the section. Artifacts have dispersed upwards as much as 55 cm and downwards as much 35 cm.

Many of the empirical features of the Barger Gulch artifact distribution may be recognized in the simple simulations presented above. In particular, the concave distributions above and below the Folsom occupation may be diagnostic of non-local mixing (compare Fig. 8 with 13e and 15). In other words, one or more mixing agents at Barger Gulch may have been active in transporting artifacts directly between non-adjacent strata. It is also reasonable to propose that Barger Gulch has experienced only early stage mixing since, under many conditions, the concave distributions generated by non-local mixing are replaced by Gaussian-like and ultimately a stable (e.g., uniform) distributions at intermediate and later stages of mixing, respectively. However, unlike in the simple simulations above, there is a global asymmetry in the vertical distribution of specimens centered on the occupation horizon. Not only have more specimens moved upwards through the section, but they also have moved over a greater vertical distance. Differences in sediment characteristics are the obvious cause and consequently modifications to the above models are necessary to account for the asymmetry.

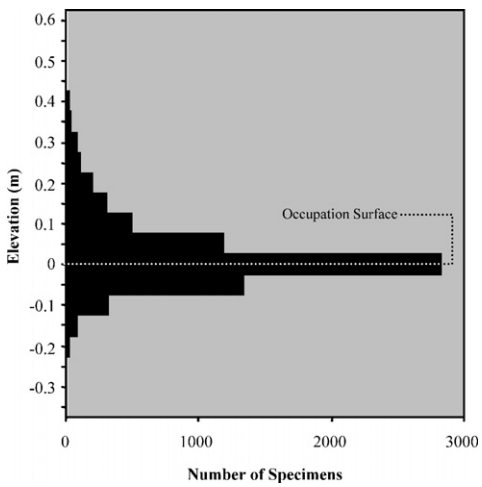

Fig. 15. Vertical frequency distribution of lithic specimens from a 75 m^2 excavation at the Barger Gulch site. The elevation of specimens (in meters) is given relative to the inferred Folsom occupation level (±0 m). Shown is the distribution for 7018 lithic specimens 10–25 mm in maximum dimension.

We simulated mixing of the Barger Gulch assemblage lithic assemblage by calibrating the model against observed artifact counts. We assume, as required by the simple models, that each specimen in the size class 10–25 mm has the same probability a_{jk} of mixing between a focal stratum j and another stratum k. Individual mixing probabilities are probably very different for specimens of different size classes (Baker 1978; Bocek 1986; Villa 1982). Surovell et al. (2005) have demonstrated that the largest artifact specimens at Barger Gulch cluster vertically at the inferred Folsom occupation horizon compared with smaller artifacts. We assume that all specimens in any given 1 m^2 excavation unit were initially deposited at the Folsom occupation surface. Therefore, all specimens start with a relative vertical elevation of ±0 centimeters. In accordance with the excavation strategy used at the site, mixing is modeled between discrete stratigraphic units each 5 cm in thickness. Thus, mixing occurs in incre-

ments of 5 cm above and below the occupation surface.

For simplicity, we also assume that there has been no horizontal movement of artifacts between excavation units subsequent to their initial burial (but see Balek, 2002; Surovell et al., 2005). There is spatial variability in the number of specimens present in any simulated vertical section (excavation unit), but the number of specimens in each vertical section is conserved over the course of mixing. For example, a vertical section starting with 23 specimens at the Folsom occupation surface will still have 23 specimens, possibly distributed over multiple stratigraphic units, after mixing. Using the Barger Gulch data, the mean number of specimens per simulated vertical section is 93.6 (median = 48) and the standard deviation is 113.3. The minimum number of specimens in any of the simulated sections is 2 (Units N1467, E2433 & N1476, E2436) and the maximum is 556 (Unit N1475, E2448).

Examination of the Barger Gulch vertical artifact distribution suggests that the most appropriate non-local mixing models has two essential features. First, we propose that the probability of mixing between non-adjacent strata decreases at a constant rate with increasing distance from the Folsom occupation surface. The corresponding probability a_{jk} is given by a negative exponential distribution (see Faure and Mensing, 2005; Surovell and Brantingham, 2007)

$$a_{jk} = a_{jl}\mathrm{e}^{-\lambda(k-1)}, \quad k = j \pm d \leqslant r \tag{9}$$

where, as above, a_{jl} is the baseline local mixing probability between focal stratum j and the next adjacent stratum above or below (i.e., $l = j \pm 1$). The parameter λ is a decay constant which drives a decline in the probability of mixing between j and k as the distance between j and k increases. The parameter d is the distance in stratigraphic units between the focal stratum j and the recipient stratum k, which at Barger Gulch corresponds to 5 cm intervals. For example, $d = 1$ applies to the probability of a single specimen moving from one stratigraphic unit to either of the adjacent units ±5 cm away. By contrast, $d = 5$ applies to the probability of mixing between one stratigraphic unit and units ±25 cm away. Note that Eq. (9) returns the baseline local mixing probability a_{jl} when $d = 1$ and that the value of a_{jk} decreases from this maximum towards zero as d increases. Finally, the parameter r is the range over which non-local mixing is allowed to occur. For example, if $r = 4$, then the maximum non-local mixing distance is between any focal stratum j and those four stratigraphic units above or below (i.e., $k = j \pm 4$). If $r = 10$, then mixing could occur between a focal stratum and strata 10 stratigraphic units above or below (i.e., $k = j \pm 10$). Mixing is not allowed between strata outside of the range of mixing. For example, if $r = 4$ then the probability of mixing between a focal stratum and one five stratigraphic units away is zero.

Second, we recognize that there is a major difference the nature of mixing above and below the inferred Folsom occupation horizon. More extensive mixing has occurred above the occupation than below. The lower permeability to mixing below the occupation surface is likely related to the well-developed Btkb soil horizon found at 0 to −5 cm (Surovell et al., 2005). We therefore allow separate model parameterizations for the stratigraphic units above (+5 to +60 cm) and below (−5 to −60 cm) the occupation surface (Table 2). In particular, we allow for a smaller decay constant ($\lambda_1 = 1$) in the strata above the Folsom occupation surface compared with the strata below ($\lambda_2 = 2$). The range of mixing is the same ($r_1 = r_2 = 6$). In practice, this means that individual specimens have a higher probability of non-local mixing in the zone above the Folsom occupation. For example, using the model parameters given in Table 2, the probability of mixing between the Folsom occupation surface and a position three stratigraphic units above is $a_{jk} = 0.00135$. Mixing between the Folsom occupation surface and a position three stratigraphic units below is $a_{jk} = 0.000025$, about two orders of magnitude less likely. These differences are driven by the different values of λ.

Figs. 16 and 17 show the results of the simulation. The exponential non-local mixing model for Barger Gulch produces mixing dynamics that parallel the example non-local mixing model in some ways (see Fig. 8). The initial stages of mixing (e.g., after 50 steps) generate a vertical distribution of specimens that is concave both above and below the occupation surface (Fig. 16). Over longer periods of time, the distribution appears more Gaussian (e.g., after 100 steps) and eventually approaches a stable form that encompasses all of the stratigraphic units (e.g., after 5000 time steps). Importantly, during the early stages of simulated mixing, the mode of the distribution remains centered on the initial occupation surface. During later stages of simulated mixing, the density of specimens follows a step function centered on the original occupation horizon.

Table 2
Barger Gulch simulation model parameters

Variable	Value	Units	Description
a_{jk}	$<a_{jl}$	Probability	Probability of single specimen mixing from j to k
a_{jl}	0.01	Probability	Baseline local mixing probability between j and the adjacent stratum above or below ($l = j \pm 1$)
λ_1	1	Stratigraphic units^{-1}	Decay constant for vertical positions above the Folsom occupation surface
λ_2	3	Stratigraphic units^{-1}	Decay constant for vertical positions below the Folsom occupation surface
r_1	6	Stratigraphic units	The maximum non-local mixing span (in stratigraphic units) for vertical positions above the Folsom occupation surface
r_2	6	Stratigraphic units	The maximum non-local mixing span (in stratigraphic units) for vertical positions below the Folsom occupation surface
e	2.718282	Scale free	Base of the natural logarithm

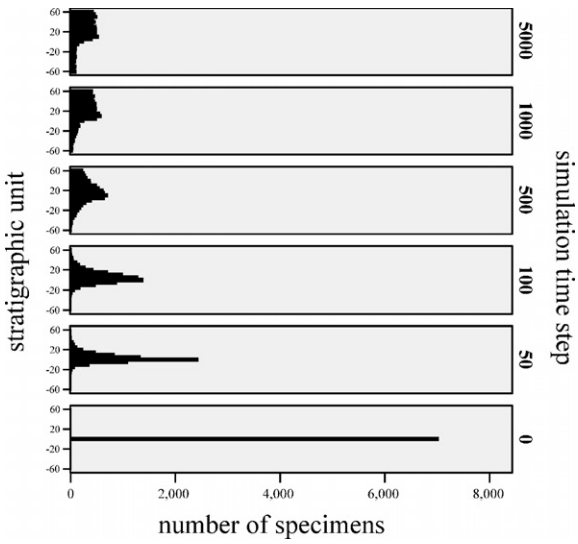

Fig. 16. Simulated mixing at the Barger Gulch site using a non-local exponential model with mixing faster in the zone above the occupation horizon. Model parameters given in Table 2.

The step distribution is clearly a product of the greater permeability of the deposits to mixing above the occupation horizon and lower permeability below. Above the occupation horizon, the late stage uniform distribution is perhaps consistent with models of an well-sorted, isotropic biomantle (Johnson et al., 2005).

Repeated simulations find a best fit between the exponential non-local mixing model and the Barger Gulch data after 41 simulated mixing events or time steps (Fig. 17a and b). The mean number of specimens remaining in the occupation stratum over ten separate simulations is very similar to the observed number at Barger Gulch (unmixed: $n_{\text{sim}} = 2826.4$, $\sigma_{\text{sim}} = 41.6$, $n_{\text{obs}} = 2830$). The mean number of specimens moving upward from the Folsom occupation in the ten simulations is slightly greater than observed (mixing up: $n_{\text{sim}} = 2710.2$, $\sigma_{\text{sim}} = 32.8$, $n_{\text{obs}} = 2419$), whereas the mean moving downward is slightly lower than observed (mixing down: $n_{\text{sim}} = 1481.4$, $\sigma_{\text{sim}} = 37.32$, $n_{\text{obs}} = 1769$). These deviations are driven primarily by differences between the model and observed distributions in the two strata immediately above the occupation surface and the one immediately below (Fig. 17b). The maximum upward movement in ten simulations is between the occupation stratum and the stratum at +55 cm, identical to that observed at Barger Gulch. The maximum downward movement in the simulations is between the occupation stratum and the stratum at −40 cm, one stratigraphic unit more than observed. Despite these differences, the two distributions are statistically very similar (Kolmogorov–Smirnov $Z = 0.566$, $p = 0.906$) (Fig. 17b). The simulation results may thus provide some support for the observations offered above, namely: (1) that the vertical movement of artifacts seen at Barger Gulch is representative of relatively early stages of non-local mixing; and (2) that the nature of the geological deposits at the site (and possibly the taphonomic agents involved) produced a significant bias against downward mixing of specimens.

There are a number of caveats that must accompany these conclusions. First, the fact that we find a good statistical fit between our model and the Barger Gulch data does not prove causation. Alternative models could be proposed to explain the observed vertical artifact distribution at Barger Gulch. For example, it is theoretically possible that the observed vertical distribution represents a case of asymmetrical mixing with the Folsom occupation surface serving as a sink for accumulation of arti-

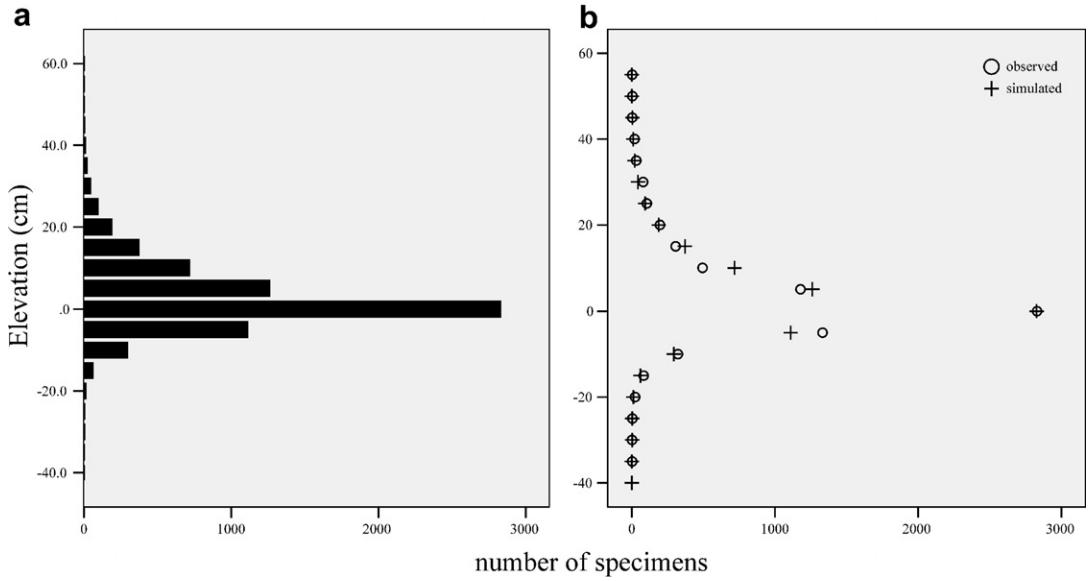

Fig. 17. Simulated mixing at the Barger Gulch site using a non-local exponential model with mixing both faster and vertically more extensive in the zone above the occupation surface. (a) Simulated vertical frequency distribution of the Barger Gulch lithic specimens ($n = 7018$) relative to the occupation surface at ± 0 (elevation in centimeters). Shown are the mean counts from 10 separate simulations in each 5 cm stratigraphic unit. (b) Quantitative comparison of simulated (+) and observed distributional data (○). See text for discussion. Model parameters given in Table 2.

facts moving with a downwards mixing bias. In this case, the Folsom occupation surface might represent a subsurface stone line in the sense of Johnson (1989). However, the pedostratigraphy, distribution of features, stone refits and, particularly, radiocarbon dates argue strongly against this interpretation (see Surovell et al., 2005). These data suggest rather that lithic specimens are mixing upwards into much younger Holocene sediments.

Second, since the model deals with mixing at a very abstract level, it is not immediately clear which specific mixing agents could be responsible for the observed and simulated patterns. Numerous disturbance agents were likely active at Barger Gulch because the site is shallowly buried and always has been (Surovell et al., 2005). Bioturbation is evident in the form of krotovina of fossorial mammals and invertebrates. Also, modern roots and rootlets of small shrubs and grasses are regularly encountered and, though no trees grow on the site today, dispersed pine charcoal and burned roots indicate the early Holocene presence of conifers, which can physically displace artifacts by root growth and during tree throw events. Cryoturbation may have affected the vertical artifact distribution as site sediments experience regular freeze–thaw cycles in the high mountain valley of Middle Park, though recent experiments suggest it probably did not play a major role (O'Brien 2006). Though clay content is fairly low (≈10%), argilliturbation may have been an important disturbance process as modern desiccation cracks occur on the surface, and identical features are occasionally encountered subsurface as well. As in many archaeological contexts, multiple disturbance agents have contributed to the observed vertical (and horizontal) spatial patterning at Barger Gulch. Since the aggregate impact of the many implicated mixing agents is uncertain, we argue that the abstract, general model presented above is appropriate for investigating mixing at Barger Gulch.

Third, while mixing above and below the Folsom occupation horizon is simulated as occurring simultaneously, it is at least possible that mixing may have occurred at different times in these two contexts; i.e., mixing below the occupation horizon may have occurred primarily in the time period between initial deposition and the inferred erosion event during the early Holocene, while mixing above the occupation horizon may have occurred primarily during late Holocene (see Surovell et al., 2005). It is also difficult therefore to be more precise than simply suggesting Barger Gulch has experienced only early stages of mixing. One would need to calibrate the time scale of mixing either based on experimental observation of different tapho-

nomic agents, or by comparing multiple sites of different ages from similar sedimentary contexts to say more than this. Neither of these alternatives are presently available for Barger Gulch.

Finally, it is clear that differences in sedimentary characteristics may have played an important role in the broad mixing dynamics at Barger Gulch. These differences were accommodated within our model by proposing that baseline mixing probabilities a_{jl} were modified by exponential functions with parameterizations favoring more extensive mixing above the occupation horizon than below. However, a more realistic model would need to include a more complete characterization of sedimentary characteristics and perhaps explicit rendering of these characteristics in the transition probability matrix (Eq. (1)).

Discussion

The simple models presented here provide a general, but rigorous approach to studying two of the primary processes involved in post-depositional mixing. Mixing of specimens out of individual stratigraphic units is described by Eq. (3), while mixing into the same units is described by Eq. (4). These are combined in a master equation that describes the simultaneous operation of both processes [Eq. (7)]. Using these equations in combination with general rules for assigning mixing probabilities between strata [Eq. (1)], it is possible to identify at a general theoretical level the common stages and patterns that may accompany post-depositional mixing (Fig. 18a).

When archaeological materials are confined to some subset of the total strata in the sequence—in other words, they form discrete occupations—then mixing may involve two stages: (1) dissipation; and (2) establishment of a mixing equilibrium. This is very apparent in the case of symmetrical local mixing of a single occupation horizon (Fig. 18a). Dissipation is signaled first by the development of a Gaussian normal distribution of specimens across stratigraphic units. This distributional pattern may be diagnostic of relatively minor amounts of symmetrical local mixing, though future empirical work is needed to verify this claim. Dissipation is predicted where the cumulative probability of mixing out from focal units with large number of specimens (e.g., the stratigraphic mode) is greater than the

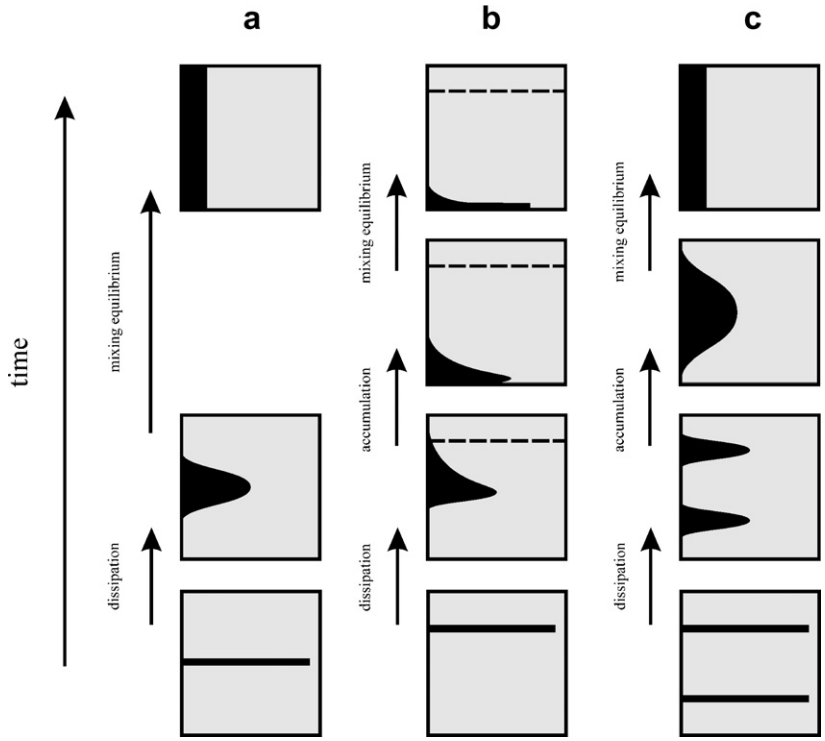

Fig. 18. Major stages in post-depositional mixing of discrete occupations. (a) Symmetrical local mixing of a single occupation horizon. (b) Asymmetrical local mixing of a single occupation horizon. (c) Symmetrical local mixing of two separate occupations.

probability of mixing in from units with small numbers of specimens (see Eq. (6)). As dissipation continues, the amplitude of the mode declines and, over long periods of time, disappears completely leaving a uniform distribution (Fig. 18a). This is a so-called mixing equilibrium since mixing may be ongoing, but it leads to no net change (beyond small stochastic fluctuations) in the number of specimens in any of the stratigraphic layers.

In cases where there is either asymmetrical mixing, or there are multiple occupation horizons in a profile, an accumulation stage may appear between dissipation and the establishment of a mixing equilibrium. In the case of asymmetrical mixing with a downward bias, for example, an initial dissipation phase is followed by gradual accumulation of specimens in the lowest unit that allows in mixing (Fig. 18b). Trailing specimens may take some time to complete their transit to base of the profile. But, when they finally do, the system arrives at a type of secular equilibrium (see Faure and Mensing, 2005); the rate of any further downward mixing is controlled by the rate at which specimens are mixed up from the bottom of the profile. A similar accumulation dynamic may also occur above the base of a section if there are major changes in sediment texture; for example, a subsurface carbonate horizon (caliche) may serve as a barrier to mixing of specimens below a certain depth (see Johnson, 1989; Shull, 2001).

Accumulation may also characterize post-depositional mixing of multiple discrete occupations (Fig. 18c). However, the cause of the dynamic in this case is quite different. In general, dissipation during the early stages of mixing may cause specimens from discrete occupations to merge, producing a unimodal distribution from a bimodal (or multimodal) distribution. A Gaussian-like normal distribution may result if the two merging distributions are themselves Gaussian. The system may shift back to dissipation, which is reflected in the progressive fall in amplitude of the single mode, and then converge on a mixing equilibrium (Fig. 18c).

Non-local mixing proceeds through all of the same general stages, though typically much faster and with different characteristic distributional shapes apparent in each stage.

The emergence of approximately Gaussian normal distributions in cases of symmetrical local mixing is not surprising since the mixing process as modeled is a simple random walk equivalent of one dimensional diffusion (Boudreau, 1997; Denny and Gaines, 2002). A Gaussian distribution also is predicted in the case of symmetrical non-local mixing if there is some limit to how far specimens can move (i.e., a maximum mixing distance). In both cases, the Central Limit Theorem applies (Denny and Gaines, 2002). Specifically, since the total distance traveled by a given specimen within a stratigraphic section is the sum of the distances traveled in each of many independent random mixing events, the aggregate distribution of distances traveled for all specimens will be approximately normally distributed. The situation becomes more complicated when we are dealing with asymmetrical local mixing. Here the appropriate comparison is with biased random walk models (Turchin 1998), which lead to normal diffusion with drift in the direction of the asymmetry.

For the simplest case of symmetrical local mixing it is also possible to specify quantitatively how the vertical spread of specimens evolves with time. Defining α as the sum of the probabilities that a single specimen is mixed from a focal stratum j to the strata immediately above or below (i.e, $\alpha = a_{jj+1} + a_{jj-1}$), then the standard deviation of the distribution of specimens after t mixing events is (Denny and Gaines 2002)

$$\sigma = \sqrt{\alpha t} \tag{10}$$

The standard deviation relative to an initial occupation horizon is proportional to the square root of the amount of time exposed to mixing. Estimates of the spread of specimens in cases of non-local mixing may also be obtained (e.g., Zanette and Alemany 1995), but their form is strongly dependent on the specific nature of the transport process.

The appearance of a uniform mixing equilibrium is also expected in cases of symmetrical mixing. This is easiest to see if we write a simplified version of Eq. (6) dealing with a focal stratum and only the two adjacent strata above and below

$$\Delta n_j = \underbrace{n_{j+1}a_{j+1,j}}_{n \text{ from stratum above}} + \underbrace{n_{j-1}a_{j-1,j}}_{n \text{ from stratum below}} - \underbrace{n_j a_{j,j+1}}_{n \text{ to stratum above}} - \underbrace{n_j a_{j,j-1}}_{n \text{ to stratum below}} \tag{11}$$

Because the mixing probabilities are symmetrical and equal in all cases we may replace the various terms $a_{j+1,j}, \ldots, a_{j,j-1}$ with a single term a_{jk}. Simplifying the resulting equation gives

$$\Delta n_j = a_{jk}(n_{j+1} + n_{j-1} - 2n_j) \tag{12}$$

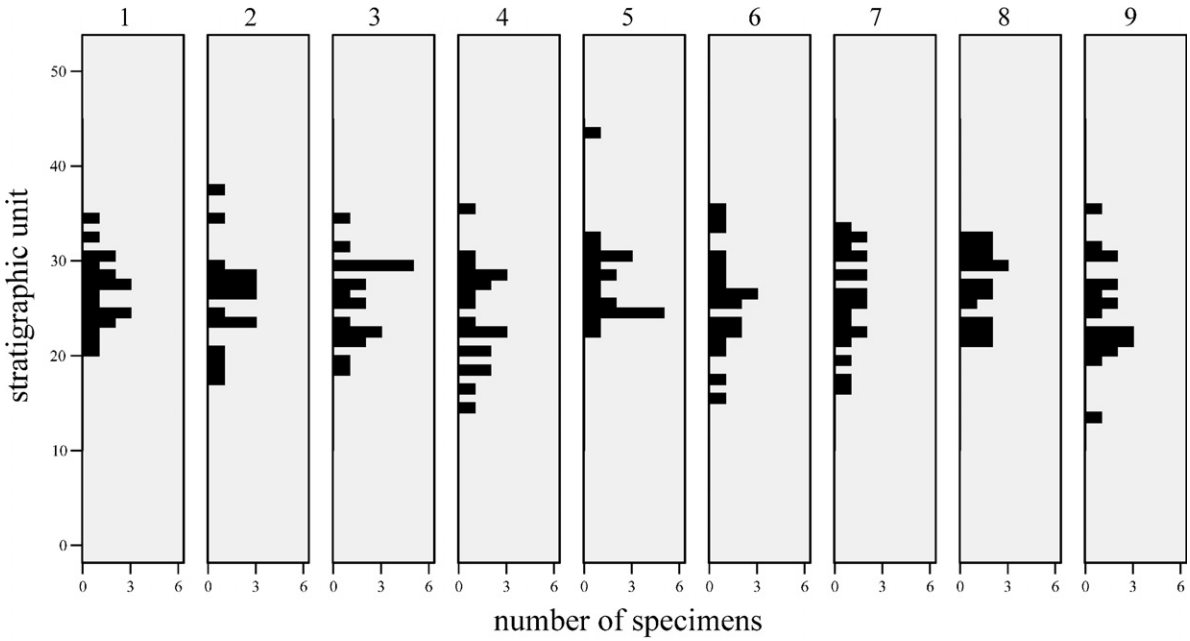

Fig. 19. Simulated symmetrical local mixing involving small numbers of archaeological specimens. Shown are the vertical distributions of specimens in ten separate sections after 500 mixing events. For large numbers of specimens the distributions should be Gaussian but are highly variable because of small sample sizes.

The system can be in equilibrium (i.e., $\Delta n_j = 0$) if $a_{jk} = 0$, meaning that there is no mixing between stratigraphic layers, or if $n_{j+1} = n_{j-1} = n_j$, meaning that there is an equal number of specimens present in each layer. In other words, the mixing equilibrium is a uniform distribution of specimens across all strata.[1] The same conclusion obtains in the case of non-local mixing provided that the mixing probabilities at distances d above and below a focal stratum are also symmetrical.

We must temper the above observations with the recognition that the small sample sizes typical of real archaeological contexts might impede our ability to recognize both different mixing systems and different mixing stages. Fig. 19 shows nine simulated vertical artifact distributions for small samples of specimens ($n = 20$) after 500 time steps of symmetrical local mixing with $a_{jk} = 0.01$, $k = \pm 1$. The expected result under these conditions is a Gaussian normal distribution of specimens centered on the initial occupation horizon (see Fig. 4). At small sample sizes, however, there is substantial variability in empirically observed patterns and individual stratigraphic sections might be easily misinterpreted. For example, in none of the nine simulated sections is there an obvious single peak in occupation intensity. In some instances (e.g., Section 1) specimens remain largely clustered vertically, suggesting continuous occupation, whereas in others there appear to be clusters with intervening occupation hiatuses (e.g., Section 9). There is also great variability in the distances over which specimens have moved (e.g., Section 1 vs. 5). In all of the sections one would be hard pressed to infer that mixing was local and symmetrical and it is not obvious whether the distributions represent a mixing equilibrium or some intermediate mixing stage. Only at larger sample sizes do these patterns become apparent.

A number of criticisms might be voiced about the research presented here and we address some of these now. First, it is important to recognize that the simulations and empirical case presented above are not meant to be exhaustive of all of possible types of post-depositional mixing that might be seen in the archaeological record. Nor is it necessarily the case that the generic mixing models considered here

[1] This is strictly true only for cases where there is no flux of specimens across the boundaries, which should hold for most stratigraphic sections and material types. Flux boundary conditions might be more appropriate for studying isotopes or organics that may be lost through the base of the section. Flux boundary conditions allow for linear decreasing or increasing equilibrium solutions.

are equally likely to occur in empirical settings. For example, it may be the case that asymmetrical mixing is far more common than symmetrical mixing in the vast majority of archaeological settings. While archaeological site formation and diagenesis is a complex, multivariate process, we also believe that there are many advantages to occasionally stepping back from a complex empirical reality to consider simple models. These are often easier to analyze and may provide a clear picture of fundamental dynamics.

Second, of the many ways in which these models might find empirical application, we opted for model-fitting as a reasonable first approach. Another approach would be to quantitatively characterize the short-term effects of different individual mixing agents and produce a calibrated transition matrix. Simulation could then be used to examine the theoretical impact of mixing by each agent type over ecological and geological time scales. Comparisons between simulations and empirical examples might reveal which of the many possible taphonomic agents were likely responsible for observed patterns. The advantage of simulation over traditional experimental approaches in this context is that ecological and geological time scales can be investigated (Wilke and Adami 2002). Unfortunately, this approach is not easily accomplished at Barger Gulch because many different mixing agents may have been active and may have had overlapping effects.

Third, it is clear that there are a number of important variables that have been excluded from the current models. These include the impact of differences in sediment characteristics on mixing (Johnson et al., 2005; Shull, 2001), variability in thickness of stratigraphic units (Meysman et al., 2003; Shull, 2001), active sedimentation and burial (i.e., advection) (Balek, 2002; Boudreau, 1997), sediment compaction (Andrews, 2006), horizontal mixing, which might occur at the surface before burial or within a sedimentary column after burial (Audouze and Enloe 1997; Enloe 2006; Surovell et al. 2005), and decay or destruction of materials as a function of time or sediment characteristics (Pendall et al. 1994; Surovell and Brantingham 2007; Trumbore 2000; Wang et al. 1996). The fact that we needed to use different model parameterizations above and below the Folsom occupation surface at Barger Gulch to arrive a reasonable description of mixing dynamics there illustrates that most empirical applications may need to move beyond the simple examples presented here. However, there are clear avenues for modeling each of these added complexities. For example, in contrast to the simulations presented above where the number of specimens is conserved over time, other types of materials (e.g., organics) might be gradually destroyed in addition to being exposed to mixing. One might incorporate time (and depth) dependent destruction of specimens by modifying Eq. (6) to read

$$\Delta n_j = \sum_{\substack{k=1 \\ k\neq j}}^{m} a_{kj} n_k - n_j \sum_{\substack{k=1 \\ k\neq j}}^{m} a_{jk} - \gamma_j n_j \tag{13}$$

where γ_j is a decay constant associated with focal stratum j. The last term in Eq. (13) thus introduces time-dependent exponential decay in the number of specimens present in stratum j. Similar modifications to Eq. (6) may allow one to consider the impact of active burial into or variable sedimentary characteristics on mixing dynamics (Boudreau 1997; Meysman et al. 2003; Shull 2001). The absence of these and other complexities from the current models, however, should not detract from the general conclusions that there may be substantial regularities that emerge from post-depositional mixing of archaeological deposits.

Conclusions

Post-depositional mixing of archaeological deposits may be modeled as a stochastic process that assigns probabilities to the event that a single specimen of a given artifact class is mixed between any two discrete stratigraphic layers. The change in the number of artifact specimens in a single stratigraphic layers is described by a simple recursion relation that includes terms for the movement of specimens both out of and into a so-called focal stratum. Mass movement of artifacts within a stratigraphic section is then the cumulative number of such mixing events between all strata.

Simulations were used to characterize symmetrical local and non-local mixing dynamics. Both processes appear to have characteristic dynamics. The early and intermediate stages of symmetrical local mixing may be recognized by the development of Gaussian-like vertical distributions of artifacts within a stratigraphic column. Symmetrical non-local mixing, by contrast, may be characterized by the development of vertical distributions of artifacts that follow closely the underlying single-specimen

probabilities of transport between strata. As in the symmetrical case, intermediate stages of symmetrical non-local mixing may be characterized by the development of a Gaussian-like vertical distributions of specimens. The vertical distributions of artifacts generated by the late stages of symmetrical local and non-local mixing are typically uniform.

Simulations were also used to characterize asymmetrical local mixing, where there is directional bias in the movement of single specimens downwards (or upwards) in the section. Here we see the development of skewed vertical distributions of specimens in section and the regular migration of the density peak (distribution mode) in the direction of the bias. The equilibrium distribution of specimens in this case shows most artifacts accumulated in the lowest (or highest, if the bias is upwards) stratigraphic unit that allows mixing. It was shown that many of these general dynamical features of post-depositional mixing appear even under more complex initial distributions of archaeological materials in section. In particular, we considered mixing of more than one discrete initial occupation and a case of an exponentially increasing distribution of artifact specimens.

Examination of the Barger Gulch Folsom site suggested that non-local mixing agents may have played a role in generating the vertical distribution of artifacts seen there. The preservation of strongly concave vertical distributions of artifacts both above and below the initial Folsom occupation is indicative of early stage mixing. It was proposed also that there is a global asymmetry characterizing mixing at the site; more extensive mixing occurred in the strata above the original occupation surface compared with below. A calibrated simulation, using a negative exponential model for the mixing probabilities, was able to statistically approximate the vertical distribution of artifacts at Barger Gulch. We view this result as preliminary support for the general validity of the models developed herein for studying post-depositional mixing of archaeological deposits.

Acknowledgments

We thank David Madsen, Charles Perreault, David Rhode, and several anonymous reviewers for their insightful comments on earlier versions of this paper. Work at Barger Gulch is supported by the National Science Foundation (BCS-0450759) awarded to Waguespack and Surovell. Any opinions, findings, and conclusions or recommendations expressed are those of the authors and do not necessarily reflect the views of the National Science Foundation.

References

Albert, R.M., Bar-Yosef, O., Meignen, L., Weiner, S., 2003. Quantitative phytolith study of hearths from the Natufian and middle palaeolithic levels of Hayonim Cave (Galilee, Israel). Journal of Archaeological Science 30, 461–480.

Andrews, B.N., 2006. Sediment consolidation and archaeological site formation. Geoarchaeology—An International Journal 21, 461–478.

Araujo, A.G.M., Marcelino, J.C., 2003. The role of armadillos in the movement of archaeological materials: an experimental approach. Geoarchaeology 18, 433–460.

Audouze, F., Enloe, J.G., 1997. High resolution archaeology at Verberie: limits and interpretations. World Archaeology 29, 195–207.

Baker, C.M., 1978. Size effect-explanation of variability in surface artifact assemblage content. American Antiquity 43, 288–293.

Balek, C.L., 2002. Buried artifacts in stable upland sites and the role of bioturbation: a review. Geoarchaeology 17, 41–51.

Bocek, B., 1986. Rodent ecology and burrowing behavior-predicted effects on archaeological site formation. American Antiquity 51, 589–603.

Bollong, C.A., 1994. Analysis of site stratigraphy and formation processes using patterns of pottery sherd dispersion. Journal of Field Archaeology 21, 15–28.

Boudreau, B.P., 1997. Diagenetic Models and Their Implementation: Modeling Transport and Reactions in Aquatic Sediments. Springer, Berlin.

Brantingham, P.J., 2007. A unified evolutionary model of archaeological style and function based on the price equation. American Antiquity 72, 395–416.

Delagnes, A., Roche, H., 2005. Late Pliocene hominid knapping skills: the case of Lokalalei 2C, West Turkana, Kenya. Journal of Human Evolution 48, 435–472.

Denny, M., Gaines, S., 2002. Chance in Biology: Using Probability to Explore Nature. Princeton University Press, Princeton.

Enloe, J.G., 2006. Geological processes and site structure: assessing integrity at a late Paleolithic open-air site in northern France. Geoarchaeology 21, 523–540.

Erlandson, J.M., 1984. A case-study in faunalturbation-delineating the effects of the burrowing-pocket-gopher on the distribution of archaeological materials. American Antiquity 49, 785–790.

Esdale, J.A., Le Blanc, R.J., Cinq-Mars, J., 2001. Periglacial geoarchaeology at the Dog Creek site, northern Yukon. Geoarchaeology—An International Journal 16, 151–176.

Faure, G., Mensing, T.M., 2005. Isotopes: Principles and Applications. John Wiley and Sons, Hoboken.

Hilton, M.R., 2003. Quantifying postdepositional redistribution of the archaeological record produced by freeze–thaw and other mechanisms: an experimental approach. Journal of Archaeological Method and Theory 10, 165–202.

Hofman, J.L., 1986. Vertical movement of artifacts in alluvial and stratified deposits. Current Anthropology 27, 163–171.

Johnson, D.L., 1989. Subsurface stone lines, stone zones, artifact-manuport layers, and biomantles produced by bioturbation

via pocket Gophers (Thomomys Bottae). American Antiquity 54, 370.

Johnson, D.L., Domier, J.E.J., Johnson, D.N., 2005. Reflections on the nature of soil and its biomantle. Annals of the Association of American Geographers 95, 11–31.

Karavanic, I., Smith, F.H., 1998. The middle/upper Paleolithic interface and the relationship of Neanderthals and early modern humans in the Hrvatsko Zagorje, Croatia. Journal of Human Evolution 34, 223–248.

Kornfeld, M., Frison, G.C., 2000. Paleoindian occupation of the high country: the case of Middle Park, Colorado. Plains Anthropologist 45, 129–153.

Kornfeld, M., Frison, G.C., White, P., 2001. Paleoindian occupation of Barger Gulch and the use of Troublesome formation chert. Current Research in the Pleistocene 18, 32–34.

Kroll, E.M., 1994. Behavioral-implications of pliopleistocene archaeological site structure. Journal of Human Evolution 27, 107–138.

Laville, H., Rigaud, J.-P., Sackett, J., 1980. Rock Shelters of the Perigord: Geological Stratigraphy and Archaeological Succession. Academic Press, New York.

Lenoble, A., Bertran, P., 2004. Fabric of Palaeolithic levels: methods and implications for site formation processes. Journal of Archaeological Science 31, 457–469.

Lyman, R.L., 2003. The influence of time averaging and space averaging on the application of foraging theory in zooarchaeology. Journal of Archaeological Science 30, 595–610.

Mayer, J.H., Surovell, T.A., Waguespack, N.M., Kornfeld, M., Reider, R.G., Frison, G.C., 2005. Paleoindian environmental change and landscape response in Barger Gulch, Middle Park, Colorado. Geoarchaeology 20, 599–625.

McPherron, S.J.P., 2005. Artifact orientations and site formation processes from total station proveniences. Journal of Archaeological Science 32, 1003–1014.

Meysman, F.J.R., Boudreau, B.P., Middelburg, J.J., 2003. Relations between local, nonlocal, discrete and continuous models of bioturbation. Journal of Marine Research 61, 391–410.

Morin, E., 2006. Beyond stratigraphic noise: unraveling the evolution of stratified assemblages in faunalturbated sites. Geoarchaeology 21, 541–565.

Morin, E., Tsanova, T., Sirakov, N., Rendu, W., Mallye, J.B., Leveque, F., 2005. Bone refits in stratified deposits: testing the chronological grain at Saint-Cesaire. Journal of Archaeological Science 32, 1083–1098.

O'Brien, M., 2006. Cryoturbation effects of upheaving on vertical deposition of lithic artifacts. Unpublished M.A. Thesis, Department of Anthropology, University of Wyoming, Laramie, WY.

Pendall, E.G., Harden, J.W., Trumbore, S.E., Chadwick, O.A., 1994. Isotopic approach to soil carbonate dynamics and implications for Paleoclimatic interpretations. Quaternary Research 42, 60–71.

Reible, D., Mohanty, S., 2002. A levy flight-random walk model for bioturbation. Environmental Toxicology and Chemistry 21, 875–881.

Rowlett, R.M., Robbins, M.C., 1982. Estimating original assemblage content to adjust for post-depositional vertical artifact movement. World Archaeology 14, 73–83.

Schiffer, M.B., 1987. Formation Processes of the Archaeological Record. University of New Mexico Press, Albuquerque.

Shull, D.H., 2001. Transition-matrix model of bioturbation and radionuclide diagenesis. Limnology and Oceanography 46, 905–916.

Surovell, T.A., Brantingham, P.J., 2007. A note on the use of temporal frequency distributions in studies of prehistoric demography. Journal of Archaeological Science 34, 1868–1877.

Surovell, T.A., Waguespack, N.M., in press. Folsom hearth-centered use of space at Barger Gulch, locality B. In: Brunswig, R.S., Pitblado, B. (Eds.), Emerging Frontiers in Colorado Paleoindian Archaeology. University of Colorado Press, Boulder.

Surovell, T.A., Waguespack, N.M., Mayer, J.H., Kornfeld, M., Frison, G.C., 2005. Shallow site archaeology: artifact dispersal, stratigraphy, and radiocarbon dating at the Barger Gulch locality B Folsom Site, Middle Park, Colorado. Geoarchaeology—An International Journal 20, 627–649.

Trumbore, S., 2000. Age of soil organic matter and soil respiration: radiocarbon constraints on belowground C dynamics. Ecological Applications 10, 399–411.

Turchin, P., 1998. Quantitative Analysis of Movement: Measuring and Modeling Population Redistribution in Animals and Plants. Sinauer Associates, Sunderland.

Van Nest, J., 2002. The good earthworm: how natural processes preserve upland Archaic archaeological sites of western Illinois, USA. Geoarchaeology—An International Journal 17, 53–90.

Villa, P., 1982. Conjoinable pieces and site formation processes. American Antiquity 47, 276–290.

Waguespack, N.M., 2005. The organization of male and female labor in foraging societies: implications for Early Paleoindian archaeology. American Anthropologist 107, 666–676.

Waguespack, N.M., Surovell, T.A., Laughlin, J.P., 2006. The 2004 and 2005 Field Seasons at Barger Gulch, Locality B (5GA195). Technical Report No. 41, George C. Frison Institute of Anthropology and Archaeology, Department of Anthropology, University of Wyoming, Laramie, WY.

Wang, Y., Amundson, R., Trumbore, S., 1996. Radiocarbon dating of soil organic matter. Quaternary Research 45, 282–288.

Wilke, C.O., Adami, C., 2002. The biology of digital organisms. Trends in Ecology and Evolution 17, 528–532.

Wood, W.R., Johnson, D.L., 1978. A survey of disturbance processes in archaeological site formation. Advances in Archaeological Method and Theory, 1.

Zanette, D.H., Alemany, P.A., 1995. Thermodynamics of anomalous diffusion. Physical Review Letters 75, 366–369.